SEM EVALUATION TO OPTIMIZE THE CONDITIONS FOR PRODUCING UNIFORM CHITOSAN NANOPARTICLES FROM SHRIMP SHELLS THAT CAN EFFECTIVELY ADSORB ACID RED 1

Fatema Tuj Jahura[1,2], Farhana Khanam Ferdousi[2], Md. Qamrul Ehsan[2], and Mohammad Abul Hossain[2*]

Article History: Received: 16.12.2023 Revised: 26.12.2023 Accepted: 26.12.2023

Abstract

Uniform chitosan nanoparticles have gained interest in recent years for their wide variety of applications. This study presents an optimum condition for preparation of uniform size of chitosan nanoparticles (CSNPs) from waste shrimp shells based on their evaluation by SEM study, and other spectrometric methods were used to characterize their adsorptive property. Initially, chitosan was extracted from shrimp shells. Then CSNPs were produced from the extracted chitosan by a self-modified ionotropic gelation method. The characteristic features of prepared chitosan and chitosan nanoparticles were investigated by determining molecular weight, degree of deacetylation, particle size, surface morphology, crystal structure, etc. using FTIR, XRD, and SEM-EDX analysis. Optimal conditions were selected based on the SEM evaluation of the uniform particles size (in a short range of 13–20 nm in diameter) of CSNPs. The adsorption efficiency of chitosan nanoparticles was investigated using acid red 1 (AR1) as a model adsorbate, and the effect of operational parameters such as contact time, dye concentration, temperature, and solution pH were investigated. Batch adsorption kinetics of AR1 on CSNPs follows pseudo second order kinetic equation. This implies the adsorption could be controlled by chemisorption, whereas the adsorption isotherms follow the Langmuir equation. The adsorption capacity of CSNPs, calculated from Langmuir equation, was found 243.9 $mg \cdot g^{-1}$ at 35 $^{\circ}C$ which escalated with increase in temperature suggesting endothermic adsorption. Based on these results, the CSNPs prepared from shrimp shell waste can be used as high potential and efficient adsorbent to remove AR1 from waste water.

Keywords: Shrimp shell, Uniform chitosan nanoparticles, SEM optimization, Characterization, Acid Red 1, Adsorption efficiency.

[1]Institute of Nuclear Science and Technology, Atomic Energy Research Establishment, Bangladesh Atomic Energy Commission, Dhaka-1349, Bangladesh
[2]Deparment of Chemistry, Faculty of Science, University of Dhaka, Dhaka-1000, Bangladesh

***Corresponding Author:** Mohammad Abul Hossain
*Email: hossainabul@yahoo.com, Email: hossainabul@du.ac.bd

DOI: 10.53555/ecb/2024.13.01.50

1. INTRUDUCTION

The shrimp processing industry is a rapidly growing concern in Bangladesh. The shells of shrimp consist of a large amount of raw shrimp weight that is discarded as waste. Hence, the shrimp industries, which are prevalent in all coastal countries, generate a massive amount of raw shrimp wastes. As shrimp shells are not soluble in nature, they take up a large portion of physical space and create pollution. Recycling shrimp shells waste and extracting commercially viable substances (such as chitin) are quick and effective ways to alleviate this problem.

Over the last few decays, the extraction of chitosan, a polysaccharide (the deacetylated derivative of chitin) from shrimp, crabs or prawns waste shells has become prominent due to its various applications. Moreover, due to its environmentally friendly nature related to green chemistry, recently, the purpose of chitosan has been the concern of fundamental research. For instance, chitosan is used as a component of wastewater treatment and also in biosensors, artificial muscles, environmentally friendly membranes, highly efficient batteries like electrolytes, etc. [1]. It also has other advantageous characteristics, such as non-antigenicity and low cost.

Chitosan can also be produced in nano and submicron sizes, since chitosan nanoparticles perform better due to their mini size and wide-reaching surface area. Moreover, they are more stable and easy to produce. In recent times many research have been reported on the formulation of nanofibers [2], nano-membranes [3], and nanoparticles (NPs) [4-5] from chitosan for using in pharmaceutical and biomedical formulations [5] due to their biocompatibility, biodegradability, and non-toxicity nature. Even NPs prepared from chitosan have applied for the delivery of antibiotics [6-7] and anti-cancer drugs [8-9] as well as for the removal of industrial effluents or dyes [10].

In this study, chitosan NPs were prepared using a self-modified ionic gelation method in which chitosan was extracted from waste shrimp shells and gelatin was applied in it with sodium tripolyphosphate. Operational conditions for the preparation of uniform chitosan nanoparticles were optimized subject to the particle size observed by scanning electron microscopy (SEM). Prepared chitosan NPs were characterized by investigating different parameters using different physicochemical methods. Then chitosan NPs were employed to remove Acid red 1 (AR1) from aqueous system as an adsorbent. The removal process was investigated by changing the operational parameters: concentration, contact time, and temperature, etc. The obtained data were correlated with different kinetic and equilibrium model equations.

2. MATERIALS AND METHOD

2.1 Chemicals

The raw shrimp shell waste (used as a source of chitosan) was collected from a local shrimp hatchery in Cox's Bazar, Bangladesh. Sodium hydroxide (NaOH), Hydrochloric acid (HCl) having a purity of 37%, Ethanol, (CH_3CH_2OH), and sodium tripolyphosphate ($Na_5P_3O_{10}$), were all procured from Merck KGaA, Darmstadt, Germany. Acetic acid (CH_3COOH) was collected from Daejung Chemicals & Metals Co. Ltd., Korea, and sodium acetate ($CH_3COONa.3H_2O$) was from Merck Specialities Private Limited, India. The AR1 dye (dye content 60%) was supplied from Sigma-Aldrich Co., USA.

2.2 Extraction of Chitosan from Shrimp Shell

Chitosan was extracted from dried shrimp shells waste following a traditional method [11] with some improved efficiency and simplicity. The collected dried shrimp shells were swept to make them free of movable tissues, washed with deionized water and dried properly. The shrimp shell was then demineralized at room temperature (RT), which involves treating it with 3% HCl for 4 hours at a shrimp shell: HCl ratio of 1:10 to remove minerals from the source. Deproteination was carried out using basic treatment with 4% NaOH solutions, at 65°-70°C for 2 h at a demineralized shell: NaOH ratio of 1:20. Then it was bleached by soaking in ethanol for 45 minutes, then clean with deionized water and dried in an oven. The resulting product is known as chitin. The chitin derived from the above processes was deacetylated using 50% NaOH at a chitin-to-NaOH ratio of 1:20 for 72 hr. at room temperature with occasional stirring. Then the product obtained was filtered, and washed out the alkalinity with deionized distilled water to receive the neutral product, and dried. The dried product is chitosan after the first deacetylation process. To get a high degree of deacetylation in chitosan, the deacetylation process was repeated with this chitosan using the same concentration of NaOH for 48 h at room temperature.

2.3 Physicochemical Characterization of Chitosan

2.3.1 Solubility

The solubility of chitosan was observed by dissolving it in acetic acid (1%) at ambient temperature. The insoluble part was filtered and dried to obtain a constant weight. Then the solubility (%) was obtained from the initial mass of chitosan and the mass of dry residue.

2.3.2 Molecular weight

The molecular weight (MW) of prepared chitosan was determined by intrinsic viscosity measurement using an Oswald viscometer. The viscometric parameters were obtained using equations (1), (2), and (3), whereas the flow time of various diluted solutions of chitosan was measured using acetate buffer as a solvent.

$$\text{Relative viscosity, } \eta_{rel} = t/t_o \quad (1)$$

$$\text{Specific viscosity, } \eta_{sp} = \eta_{rel} - 1 \quad (2)$$

$$\text{Reduced viscosity, } \eta_{red} = \eta_{sp}/C \quad (3)$$

where t_o and t are the flow times of the solvent and chitosan solutions, respectively, and C is the concentration of chitosan. The intercept obtained from the extrapolation of the plot of reduced viscosity vs. chitosan concentration (C) represents the intrinsic viscosity. Then, the Mark-Houwink equation (4) [12] was used to calculate the MW of prepared chitosan.

$$\eta = KM_v^{\alpha} \quad (4)$$

where M_v is viscosity average molecular weight, K and α are constants, the values of which depend on the polymer type and the chosen solvent.

2.3.3 Degree of deacetylation

The degree of deacetylation (DDA) of the extracted chitosan was calculated using data from the FTIR spectra of chitosan using the absorption bands at 1320 cm^{-1}, which is the characteristic of amide, which means the acetylated amine, and the band at 1420 cm^{-1} as the reference band. Finally, the following equation (5)[13] was used to calculate the DDA of prepared chitosan:

$$\%DDA = 100 - \frac{(A_{1320}/A_{1420}) - 0.3822}{0.03133} \quad (5)$$

2.4 Preparation of Chitosan Nanoparticles and Optimization of Parameters

A modified methodology was followed to prepare CSNPs which involved the gelation of chitosan solution with sodium tripolyphosphate (Na-TPP) [14]. In brief, a specific weight of chitosan was used to prepare different concentrated chitosan solutions in 1% acetic acid. An aqueous solution of Na-TPP was also prepared at a concentration of 0.25% (w/v), 1% (w/v), and 2% (w/v). The Na-TPP solution was mixed dropwise to the different chitosan solutions (chitosan-to-TPP ratio of 5:1) at room temperature under constant magnetic stirring using a magnetic stirrer (AGE Magnetic Stirrer, VELP Scientifica) for 30 min. An opalescent suspension was observed with the formation of CSNPs when Na-TPP was mixed with the chitosan solution. The suspensions were centrifuged for 15 minutes, and the CSNPs were repeatedly rinsed with distilled water. Finally, the NPs of chitosan were dried in a Freeze Drier (Labconco, USA) (temperature: -50 ^{o}C, vacuum: 0.340 mbar) to obtain dried chitosan NPs.

2.5 Spectrometric Characterization of Chitosan and Chitosan Nanoparticles

The crystalline state of synthesized chitosan and chitosan NPs was observed using an X-ray diffractometer with a CuK_{α} radiation (XRD-6000, Shimadzu, Japan) source having a wavelength of 1.5406 A^{o}. The FTIR (Fourier transform infrared) spectra of the prepared materials were recorded with an IR Prestige-21 (Shimadzu, Japan) by using the KBr disk method within the range of a frequency from 400 to 4000 cm^{-1}. The percentage of elements in chitosan was determined by an elemental analyzer (vario MICRO CHNS). Morphological characterization and particle size determination of the nanoparticles were performed by a scanning electron microscope (SEM), equipped with an energy dispersive X-ray (EDX), a field emission scanning electron microscope (FESEM), and a digital microscope (Trinocular microscope with photographic attachment, B 383P1 and CB 18, Optika, Italy).

2.6 Adsorption Study

The aqueous solution of Acid red 1 (AR1) was prepared by dissolving AR1 in distilled water. The optimum pH of solution for the adsorption was selected by monitoring the change of pH during the adsorption at different initial pH (2.0-8.0) of solutions. For adsorption kinetic study, a specific amount of chitosan NPs as an adsorbent was added to a fixed volume of solution of two different concentrations. Then solutions were shaken in a thermo stated mechanical shaker (NTS-4000A, Japan) at a fixed temperature. The adsorption of AR1 on CSNPs was performed for different contact times. After a specific contact time, the CSNPs were separated from solutions by centrifugation. A double beam UV-vis spectrophotometer "UV-1800 Spectrophotometer, Shimadzu, Japan" was used to measure the concentrations of AR1 in different solutions, before and after adsorption of AR1. The equilibrium adsorption isotherms were constructed from the effect of initial AR1 concentration at two different temperatures using predetermined

equilibrium time (3 hours) like as kinetic study. The influence of solution pH on amount adsorbed was studied by performing equilibrium adsorption experiments at various initial pH of solution. The pH of solution was measured by using a microprocessor pH Meter (pH 210, HANNA Instruments). The equation (6) and (7) were used to determine the amount adsorbed at time t (q_t), and equilibrium amount adsorbed (q_e).

$$q_t = \frac{C_0 - C_t}{M} \times V \quad (6)$$

$$q_e = \frac{C_0 - C_e}{M} \times V \quad (7)$$

where, C_o: initial concentration, C_t: concentration at time t, and C_e: concentration at equilibrium time t_e of AR1 solution (mg·L^{-1}). M is the mass of adsorbent (g) and V is the volume of AR1 solution (L) taken for conducting adsorption experiments.

3. RESULTS AND DISCUSSION

3.1 Chitosan Yield

Chitosan was extracted from wasted shrimp shells using a conventional method with some improvements in efficiency and simplicity. In this extraction process, de-mineralization and de-proteinization of shrimp shells were carried out to get chitin, followed by deacetylation of chitin to receive chitosan from raw shrimp shells. During the extraction process of chitosan, only deacetylation used a longer treatment time as it was the only process without complicated requirements such as nitrogen purging, autoclave conditions, or high-temperature reflux [15]. Figure 1 represents the extraction process of chitosan from the waste shell of shrimp. The yield of chitosan in percent was determined from the dry weight of chitosan, derived from the dried shell of shrimp. During the extraction process, at first, 14.38 g of de-mineralized shrimp shells were produced from 50 g of the dried shell by the de-mineralization step (yield: 28.76%). Then the deproteination was carried out to obtain chitin (amount of chitin: 12.5 g). The double de-acetylation of chitin gives chitosan as final product. The amounts were 5.24 g and 4.09 g after the first and second deacetylation, respectively. Thus, from 50 g of shrimp shell, 4.09 g of chitosan was obtained (the yield of chitosan from shrimp: 8.18%). The yield was in compliance with the previous literature value [16]. Indeed, the extraction process was successful to escalate the amount of product CSNPs, and finally, about 615 g of raw shrimp shells were treated according to the same method step by step, and about 45 g of chitosan was obtained and stored for characterization and uses in the production of chitosan nanoparticles and other studies.

3.2 Physiological and Functional Properties of Chitosan

3.2.1 Solubility

The solubility of chitosan obtained was 82.85% in 1% acetic acid. In comparison to the previous study, it may vary from 17.43 to 95.29% with an average of 57.52% [18]. The lower solubility is because of the 'incomplete removal of the acetyl group from chitin', which means a lower degree of deacetylation (DDA) [19]. Therefore, the higher solubility obtained in this study indicates that the extracted chitosan contains

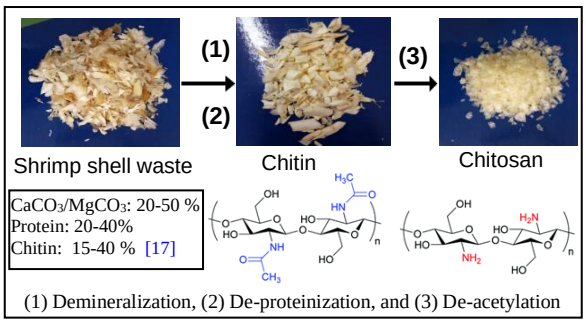

Fig. 1 Extraction of chitosan from shrimp shell waste.

A high content of amino groups, and allow chitosan to dissolve in an acidic solution through the protonation of amino groups. So, the produced chitosan has a higher DDA value, which means that better chitosan has been produced.

3.2.2 Molecular weight

The viscosity-average molecular weight (M_v) was derived from $[\eta] = KM_v^{\alpha}$, where $K = 1.424\times10^{-5}$ (dm^3/g) and $\alpha = 0.96$ for chitosan in the solvent of 0.2 M CH_3COOH/0.1 M CH_3COONa. The molecular weight of the prepared chitosan was determined to be 2.3×10^5 Da, which is in the range found in previous studies [20]. Depending on the various parameters during production, such as concentration of alkali, source, temperature, reaction time, dissolved oxygen concentration, residual aggregates in the solution, chitin concentration, the molecular weight of chitosan and shear stress may be varied [21]. The range of molecular weight of chitosan is from 10,000 Da to 250,000 Da and is classified as "low molecular weight chitosan" [22]. So, the extracted chitosan in this study is of low molecular weight.

3.2.3 Elemental analysis

The elemental analysis results of prepared chitin and chitosan are presented in Table 1. As most of the $NHCOCH_3$ groups of chitins are converted to NH_2 groups in chitosan, the percentage of carbon will be lower in chitosan than in chitin, and similarly, the C/N ratio will also be reduced. From Table 1, it is seen that chitosan exhibits a

significant reduction in the percentage of carbon as well as in the ratio of C/N compared to chitin, which indicates the deacetylation of chitin to produce chitosan.

Table 1 Elemental composition of carbon, hydrogen, nitrogen, and the ratio of C and N for chitin and chitosan

Sample	N (%)	C (%)	H (%)	C/N ratio
Chitin	6.02	42.84	3.916	7.1107
Chitosan	7.57	39.59	4.123	5.2282

3.2.4 Degree of deacetylation (DDA)

FTIR spectroscopic study was performed to determine the DDA of prepared chitosan. Figure 2 represents the FTIR spectra of extracted chitin and chitosan. The FTIR spectra of chitosan present a strong absorption band at 3421 cm^{-1} due to OH and NH groups stretching vibrations, and intermolecular hydrogen bonding. A peak at 2878 cm^{-1} is for the symmetric stretching vibration of -CH attributed to the pyranose ring. The peaks located at 1657 and 1595 cm^{-1} are assigned to -C=O stretching vibration for amide I band, and NH bending vibration for amide II band, respectively. The observed sharp peak at 1379 cm^{-1} is due to CH_3 in the amide group. Peaks at 1077 and 1027 cm^{-1} are attributed to skeletal vibrations involving C-O stretching. Now, compared with the spectrum of chitin, the major differences in FTIR spectra lie in the regions of N-H and C=O vibrations. Actually, the conversion of chitin to chitosan occurs by converting the acetyl group of chitins into an amino group, which reduces the amide content. This reduction of the amide group is observed by the reduction of two peaks at 1560 cm^{-1} and 1316 cm^{-1}. From spectra, the representative peak at 1560 cm^{-1} which is for -NH bending vibration of the $NHCOCH_3$ group, and 1316 cm^{-1} which is for complex vibration due to the -NHCO group, are significantly decreased after deacetylation of chitin with a new sharp peak for NH_2 bending vibration that appears at 1595 cm^{-1}. This confirms the conversion of chitin to chitosan.

The DDA of prepared chitosan was analyzed by applying the FTIR method of Analysis. The DDA of extracted chitosan was calculated by using equation (5) by matching the identification bands of chitosan in FTIR spectra and was found to be

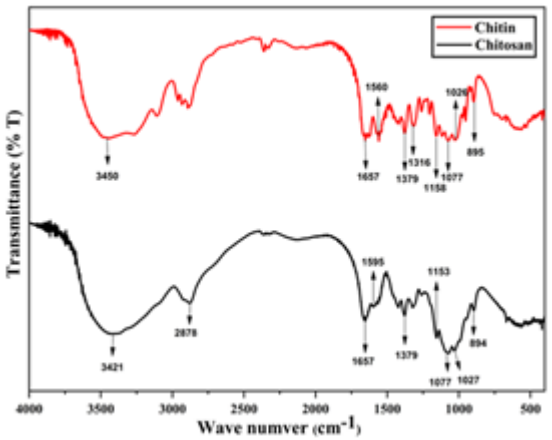

Fig. 2. FTIR spectra of extracted chitin and chitosan.

70%, which is supported by various studies [16]. The DDA values can be different for chitosan extracted from different sources and also due to the different parameters or conditions used during the deacetylation process.

3.3 Optimization of the Production of Chitosan Nanoparticles

Chitosan nanoparticles (CSNPs) were prepared by physical treatment during the incorporation of tripolyphosphate (TPP) with chitosan in different ratios. The effect of TPP and chitosan concentrations on CSNP formation and size was studied using SEM for five different CSNP formulations, as shown in Table 2. Three types of phenomena were observed in this product of formulation: (i) clear solution (CS01-CS02), (ii) opalescent suspension (CS03-CS04) and (iii) aggregation (CS05), and the latter denotes the completion of the nanoparticle formation process. For CS03, CS04, and CS05 formulations, at a chitosan and TPP mass ratio of 5:1, with different concentrations of TPP, the formation of opalescent suspension and aggregation indicated the production of chitosan particles. These three types of particles were investigated under SEM at three different magnifications (X2,000, X50,000, and X100,000) for each case and are presented in Figure 3. Based on these findings, formulation CS04 is considered an optimum condition for the production of high-quality CSNPs (particle sizes: 13-20 nm), as opposed to formulations CS03 and CS05, which have particle sizes: 96-115 nm and 113-173 nm, respectively.

3.4 Characterization of Chitosan Nanoparticles

3.4.1 SEM analysis

The surface morphology and particle size of prepared CSNPs, using the CS04 formulation, were characterized by a FE-SEM. Figure 4(a) shows the uniformly spherical nanoparticles at high magnification (X2,00,000). Because of their larger surface area to volume ratio, smaller particles may have high surface properties such as adsorption capacity, for which the formulation CS04 has been considered the optimized formulation of CSNPs preparation.

3.4.2 EDX analysis

The elemental composition of prepared CSNPs using the CS04 formulation was determined by EDX connected with SEM (Figure 4b), whose results confirm the existence of the C, N, and O with an atomic weight of 78.01%, 3.11%, and 16.53%, respectively, as the elements of chitosan. The presence of Na with an atomic weight of 0.49% and P with an atomic weight of 1.83% confirms the successful formation of CSNPs from the combination of chitosan and TPP.

3.4.3 Digital microscopic analysis

The large-scale surface structure of prepared CSNPs was investigated using digital microscopic analysis. Figure 5 shows a photograph of the surface structure of CS04-formulated CSNPs at 100 times magnification. Such observations give a preliminary idea about the existence of small particles on the surface compared with the other two formulated (CS03 and CS05) products of chitosan particles.

Table 2 Effect of concentration of chitosan and TPP on chitosan nanoparticles formation

Formulations	Factors			Results	Remarks
	Chitosan concentration (%)	TPP concentration (%)	Chitosan: TPP		
CS01	0.5	0.25		Clear solution	Particle not formed
CS02	0.5	1		Clear solution	Particle not formed
CS03	2	0.25	5:1	Opalescent suspension	Particle formed
CS04	2	1	5:1	Opalescent suspension	Particle formed
CS05	2	2	5:1	Aggregation	Particle not formed

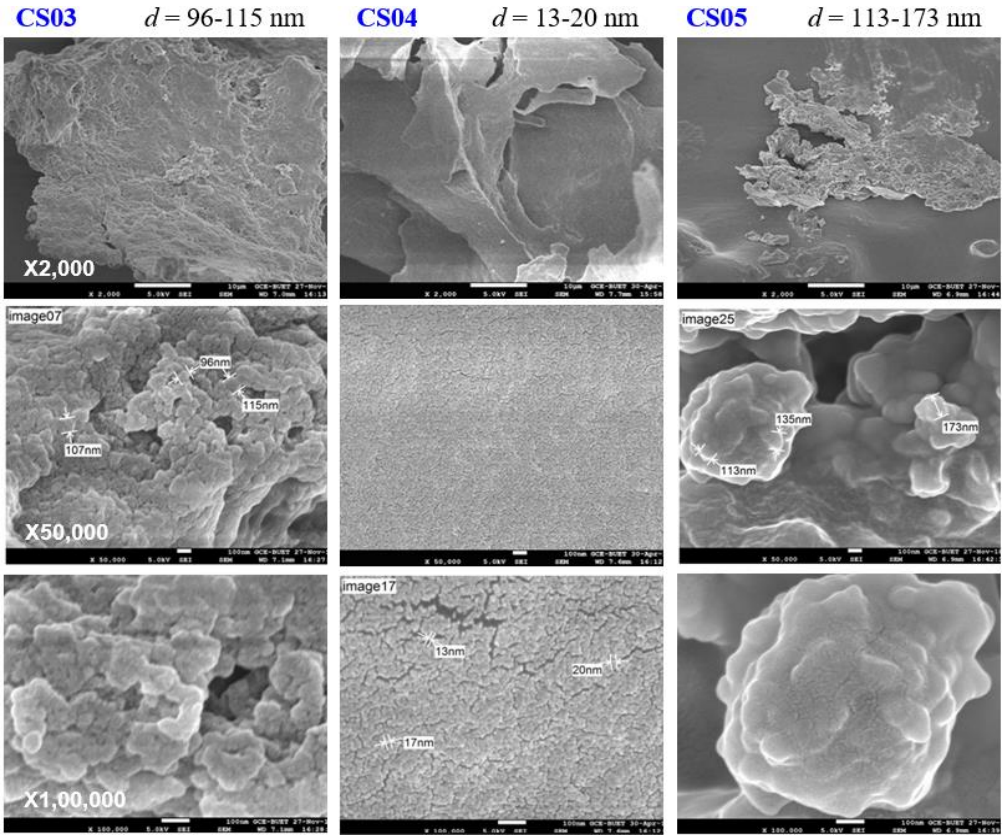

Fig. 3 SEM micrographs of chitosan nanoparticles prepared from different concentrations ratio of chitosan and TPP

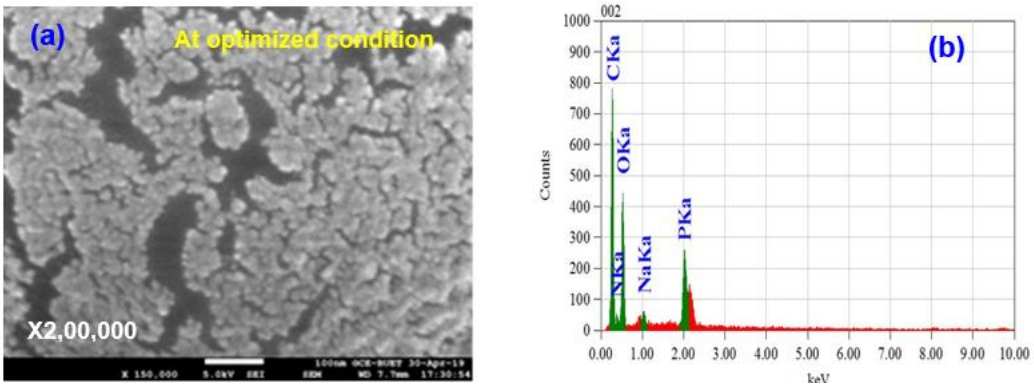

Fig. 4 SEM micrograph at high magnification (a) and EDX spectrum (b) of CSNPs of CS04 formulation

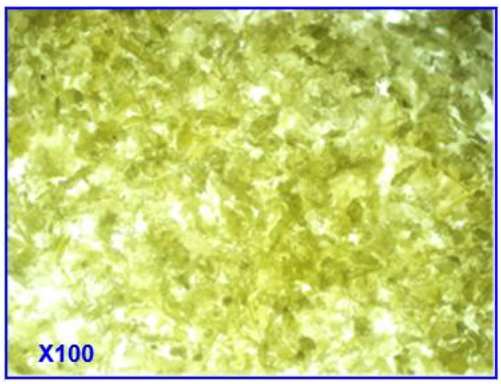

Fig. 5 Digital microscopic picture of prepared CSNPs.

3.4.4 FTIR analysis

Figure 6 represents the FTIR spectra of extracted chitosan and the CSNPs obtained from it. Comparing the FTIR spectrum of chitosan with CSNPs one, the pure chitosan was characterized by peaks located at 3421, 1657, 1595, 1417, 1077, 1027, and 894 cm^{-1}. In CSNPs, the characteristic peaks are quite similar, except the peaks located at 1657 cm^{-1}, which relates to C=O stretching in the amide group shifted to 1647 cm^{-1} and the peak at 1595 cm^{-1}, which relates to NH_2 bending in the amino group shifted to 1540 cm^{-1}. The reduced stretching frequency may be assigned to the interaction of amino group of chitosan with TPP.

3.4.5 XRD analysis

The XRD patterns of extracted chitosan and CSNPs are illustrated in Figure 7, which shows two characteristic peaks at 2θ around 10.224°, 20.357° and a shoulder peak in 22.491°, in accordance with earlier reports, which correspond to the (020), (110), and (120) planes, respectively [23, 24]. These broad diffraction peaks in the XRD pattern of chitosan represent the extracted chitosan as semi-crystalline [25].

The XRD pattern of CSNPs showed broad diffraction peaks at 2θ-scattered angles of 12.02°, 19.11° and 21.62°. The intensity of these crystalline peaks was decreased in comparison with pure chitosan. The lowering in intensity of the (110) and (020) planes of CSNPs reflected that the native chitosan had been successfully transformed into nanoparticles. Thus, the formation of nanoparticles leading to destroyed the crystal structure of chitosan, which indicates the increased amorphous nature of the nanoparticles formed.

3.5 Adsorption of AR1 on CSNPs

3.5.1 Optimum pH for adsorption

The adsorptive removal of AR1 from solution was observed at four different pH Values. The pH of

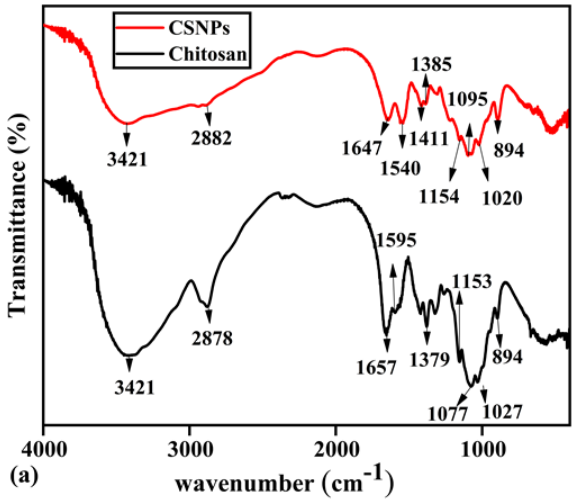

Fig. 6 FTIR spectra of chitosan and CSNPs

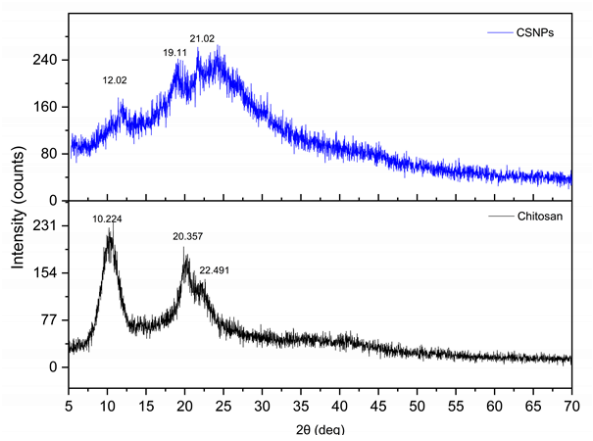

Fig. 7 XRD pattern of chitosan and CSNPs

the AR1 solution was measured before and after adsorption. The change of pH is presented by ΔpH and minimum change in pH is required for adsorption study. Figure 8 shows that when the initial pH of AR1 solution is 6.0, after adsorption the solution pH remains nearly unchanged (ΔpH~0). In the case of other pH, there is larger pH changes occurred. Subsequently, pH 6.0 was considered as an optimum pH for the further experiments of adsorptive removal of AR1 by CSNPs.

3.5.2 Adsorption kinetics

Batch adsorption experiments were performed to investigate the adsorption kinetics for different concentrations of AR1 by varying the contact

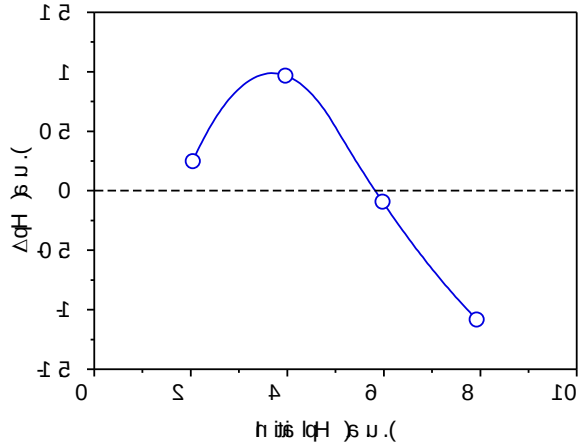

Fig. 8 Optimization of pH for the study of adsorption of AR1 on chitosan nanoparticles

time. Different kinetic models such as Lagergren's pseudo first order, Ho's pseudo second order and Weber-Morris intraparticle diffusion model were applied to the experimental results to describe the nature of adsorption kinetics. The linearized forms of these kinetic equations are expressed by equations (8), (9) and (10), respectively [26]:

$$\ln(q_e - q_t) = lnq_e - k_1 t \quad (8)$$

$$\frac{t}{q_t} = \frac{1}{k_2 q_e^2} + \frac{t}{q_e} \quad (9)$$

$$q_t = k_i t^{0.5} + C_i \quad (10)$$

where, q_t and q_e are the amount adsorbed (mg·g^{-1}) at time t and equilibrium time, respectively, C_i is the initial concentration (mg·L^{-1}), k_1, k_2 and k_i are the rate constants of pseudo-first order model (g·mg^{-1}·min^{-1}), pseudo-second order model (g·mg·g^{-1}), and intraparticle diffusion model (mg·g^{-1}·min$^{-0.5}$), respectively. Figures 9a-c show the different kinetic models which were fitted with the data obtained from the adsorption experiments performed at different contact time. Calculated values of parameters for different kinetic equations are presented in Table 3. Considering the regression factor or correlation coefficient (R^2) values of these three kinetic models, the experimental data are well fitted to the pseudo

Table 3 The kinetic parameters obtained from different models for the adsorption of AR1 on CSNPs at pH 6.0.

Kinetic model	Initial concentration (mg L^{-1})	Parameters	Value	R^2
Pseudo first order	51.2	q_e (mg·g^{-1})	111.097	0.807
		k_1 (g·mg^{-1}·min^{-1})	- 0.077	
	10.1	q_e (mg·g^{-1})	60.928	0.861
		k_1 (g·mg^{-1}·min^{-1})	-0.089	
Pseudo second order	51.2	q_e (mg·g^{-1})	71.429	1.000
		k_2 (g·mg^{-1}·min^{-1})	0.005	
	10.1	q_e (mg·g^{-1})	21.459	1.000
		k_2 (g·mg^{-1}·min^{-1})	0.082	
Intraparticle diffusion	51.2	k_i (mg·g^{-1}·$min^{-0.5}$)	0.966	
		C_i (mg·g^{-1})	58.408	
	10.1	k_i (mg·g^{-1}·$min^{-0.5}$)	0.049	
		C_i (mg·g^{-1})	20.763	

second order kinetic equation of highest value of R^2 indicating the rate determining step may be controlled by chemical interaction of two active sites of AR1 to the CSNPs surface which involves the exchanging or sharing of electrons between adsorbent and adsorbate [27]. According to previous studies, the adsorbent with heterogeneous surface [28-30] follows pseudo-second order kinetics. The nature of the plot of intraparticle diffusion model suggested that the rate determining step is controlled by intraparticle diffusion.

3.5.3 Adsorption isotherm

Adsorption is generally described by adsorption isotherm which is the plot of equilibrium amount of adsorbate adsorbed on adsorbent as a function of equilibrium concentration of adsorbate at a constant temperature. The adsorption isotherm was constructed by varying the AR1 concentration from 10.2 to 127.5 mg·L^{-1} at 35 and 45 ºC temperatures. The experimental data were fitted to linearized form of Langmuir, Freundlich and Tempkin isotherm models which are represented by equation (11), (12) and (13), respectively [31-32].

$$\frac{C_e}{q_e} = \frac{C_e}{q_m} + \frac{1}{K_L q_m} \quad (11)$$

$$lnq_e = lnK_F + \frac{1}{n} lnC_e \quad (12)$$

$$q_e = \frac{RT}{b} lnK_T + \frac{RT}{b} lnC_e \quad (13)$$

where, C_e = equilibrium concentration of adsorbate (mg·L^{-1}), q_e = equilibrium amount adsorbed at per unit mass of adsorbent (mg·g^{-1}), q_m = equilibrium adsorption capacity for complete monolayer (mg·g^{-1}), K_L = Langmuir adsorption constant, K_F = Freundlich adsorption constant (L·g^{-1}), T = temperature (K), n = constant related to adsorption intensity, b = constant related to the heat of adsorption (J·mol^{-1}), R = universal gas constant (8.314 J·mol^{-1} K^{-1}), and K_T = equilibrium binding constant corresponding to the maximum

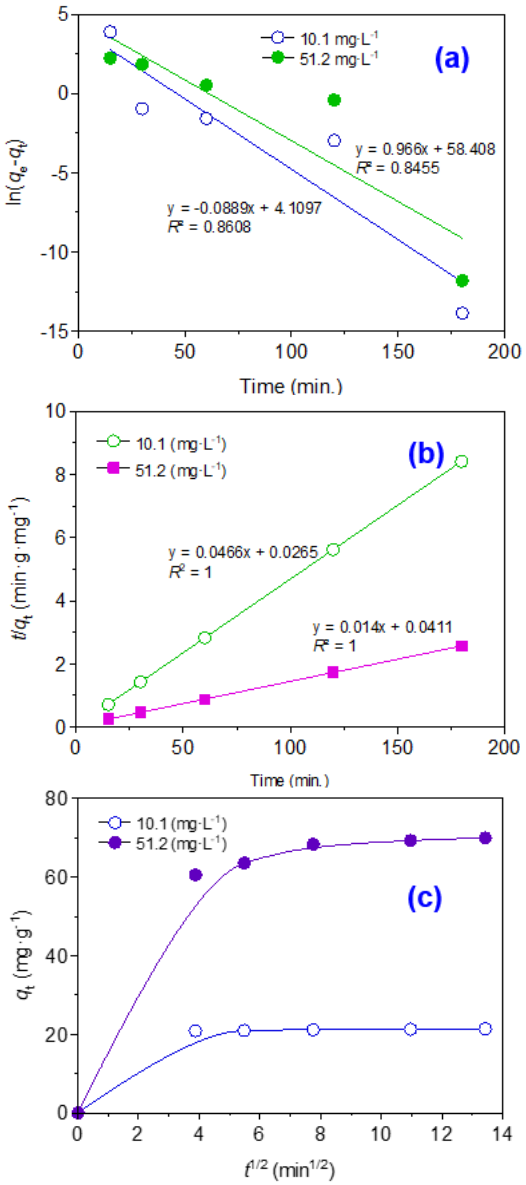

Fig. 9 (a) Pseudo-first order, (b) pseudo-second order, and (c) intraparticle diffusion models for the adsorption of AR1 on chitosan nanoparticles (pH: 6.0, CSNPs: 0.4 g·L^{-1}, shaking rate: 150 rpm, and temperature: 35º C).

binding energy ($L \cdot g^{-1}$). Figure 10(a) shows the adsorption isotherm of AR1 on CSNPs at two different temperatures. Figure 10(b-d) represents the linear forms of these three isotherm models fitted with the experimental data of adsorption isotherm at 35 ºC and 45 ºC. Different parameters were calculated and given in Table 4. Comparing the R^2 values of these three isotherm models, it shows that the Langmuir isotherm (R^2 = 0.9765 and 0.9503) is suitable for describing adsorption of AR1 on CSNPs in comparison to the Freundlich and Temkin isotherm model at both the temperatures. By reason of, the adsorption isotherm follows the Langmuir isotherm model, there is high possibility of being monolayer adsorption of AR1 on homogeneous sites of CSNPs. The adsorption capacity (q_m) of CSNPs to AR1, calculated from Langmuir equation, was found to be 243.9 $mg \cdot g^{-1}$ at 35 ºC which is increased with increase in temperature, and q_m = 333.3 mg·g-1 at 45 ºC. Such effect of temperature is indicating the endothermic nature of the adsorption, which is mostly for chemisorption. In previous studies, CSNPs showed higher adsorption capacity compared to the other adsorbents for adsorption of AR1. In a study reported by Munilakshmi [33], the adsorption capacity of Aluminium Sulphate, Ferric chloride and Ferrous slphate flocs for AR1 was 32.26 $mg \cdot g^{-1}$, 250 $mg \cdot g^{-1}$ and 6.623 $mg \cdot g^{-1}$, respectively. Thus CSNPs has an excellent adsorbent to remove AR1 from aqueous solutions.

4. CONCLUSION

Chitosan was successfully prepared from shrimp shell wastes with a DDA value of 70% and a molecular weight of 2.3×10^5 Da. Then chitosan nanoparticles (CSNPs) were formulated from chitosan by modified ionic gelation of chitosan with TPP. SEM characterization of surface morphology and particle size of CSNPs showed that the concentration of

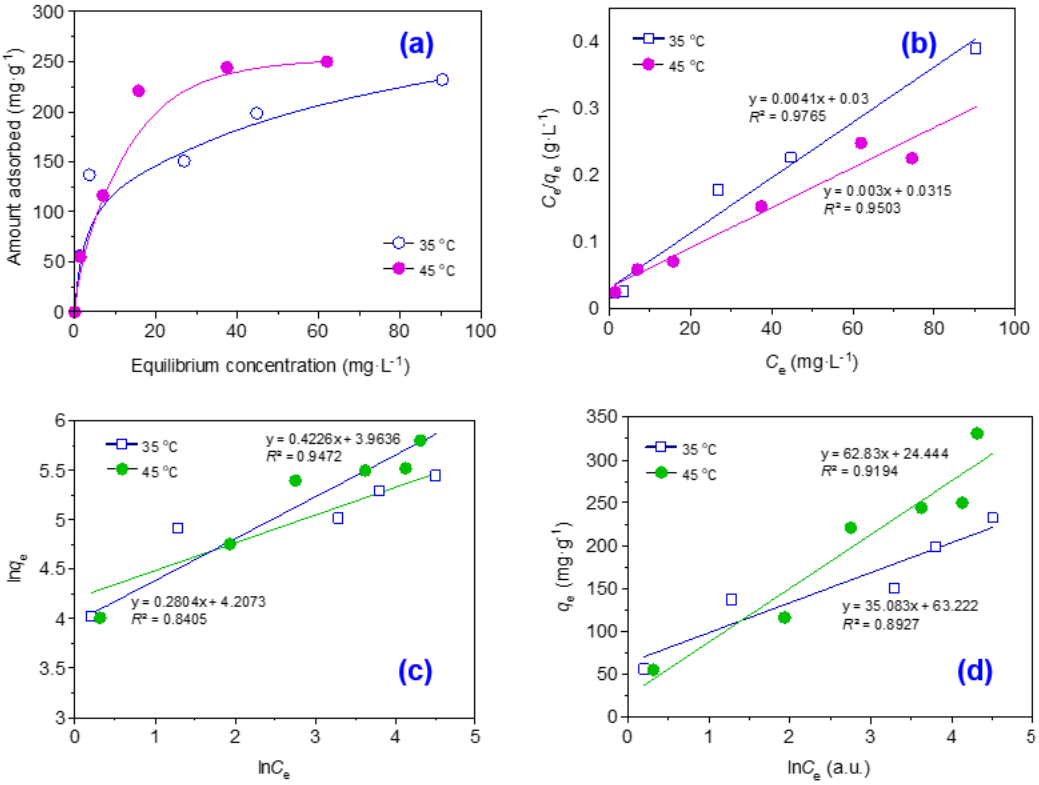

Fig. 10 (a) Adsorption isotherm (b) Langmuir isotherm, (c) Freundlich isotherm and (d) Temkin isotherm for AR1 adsorption on chitosan nanoparticles at different temperatures (C_o : 10.2-127.5 $mg \cdot L^{-1}$, pH: 6.0, CSNPs : 0.4 $g \cdot L^{-1}$, equilibrium time : 3 hrs., shaking rate: 150 rpm).

Table 4 Parameters obtained from Langmuir, Freundlich and Temkin isotherms for AR1 adsorption on chitosan nanoparticles at different temperatures

Isotherm model	Parameters	Unit	35ºC	45ºC
Langmuir	q_m	$mg \cdot g^{-1}$	243.9	333.3
	K_L	$L \cdot mg^{-1}$	0.137	0.095
	R^2		0.977	0.950
Freundlich	K_F	$L \cdot g^{-1}$	67.18	52.65
	n		3.566	2.366
	R^2		0.805	0.947
Temkin	K_T	$L \cdot g^{-1}$	5.273	1.476
	b	$J \cdot mol^{-1}$	72.99	40.76
	R^2		0.893	0.919

Chitosan and TPP affected the formation of nanoparticles. According to the results, 2% chitosan with 0.25% TPP-initiated ionic gelation and produced uniformed CSNPs with the range of particle size: 13-20 nm which was considered the optimal condition for the formation of desired uniformed chitosan nanoparticles. The adsorption efficiency of CSNPs to AR1 was investigated in batch process. The adsorption kinetics follows the pseudo-second order model indicating chemisorption of AR1 on CSNPs at pH 6.0. The adsorption isotherm is well expressed by Langmuir model suggesting the adsorption of AR1 on CSNPs is probably monolayer. The maximum adsorption capacity is 243.9 $mg \cdot g^{-1}$ at 35 ^oC which increased with increase in temperature, mentioning the endothermic nature. Eventually, the prepared CSNPs seemed to have promising potentiality as an adsorbent and can be utilize as an effective and efficient adsorbent in removal of industrial dye from aqueous solution. Beyond any doubt, by reusing and recycling the shrimp shells wastes to prepare this type of CSNPs can also be a potential as well as greener solution to reduce huge amount of solid wastes from the shrimp industries. Hence this trend of waste utilization can save our natural coastal resources, energy and cost.

Acknowledgment

The authors would like to acknowledge the Centennial Research Grant (CRG: 2020-2021) of Dhaka University, for financial support to perform the research work. Fatema Tuj Jahura also thanks the Bangladesh Atomic Energy Commission (BAEC) and the Bangabandhu Science and Technology Fellowship Trust, Bangladesh, for partial financial support.

Conflict of Interest

The authors declare that they have no conflict of interest.

References

1. Zhang Q M, Furukawa T, Bar-Cohen Y, Scheinbeim J. Electroactive polymers, Materials research society symposium proceedings, Materials Research Society, Washington, D.C. 2000.
2. Geng X, Kwon O H, Jang J. (2005) Electrospinning of chitosan dissolved in concentrated acetic acid solution. *Biomaterials*, 26:5427- 5432.
3. Cathell M D, Szewczyk C, Frances A B, Carrie A. W, Wolever J D, Kang J, Schauer C L. (2007) Structurally colored thiol chitosan thin films as a platform for aqueous heavy metal ion detection. *Biomacromolecules,* 9(1):289-295.
4. Oyarzun-Ampuero F A, Brea J, Loza M I, Torres D, Alonso M J. (2009) Chitosan-hyaluronic acid nanoparticles loaded with heparin for the treatment of asthma. *Int J Pharmaceutics*, 381(2):122-129.
5. Li X, Han Y, Ling Y, Wang X, Sun R. (2015) Assembly of layered silicate loaded quaternized chitosan/reduced graphene oxide composites as efficient absorbents for double-stranded DNA. *ACS Sustainable Chem. Eng*., 3(8):1846-1852.
6. Cover N F, Lai-Yuen S, Parsons A K, Kumar A. (2012) Synergetic effects of doxycycline-loaded chitosan nanoparticles for improving drug delivery and efficacy. *Int J Nanomedicine*, 7:2411–2419.
7. Saha P, Goyal A K, Rath G. (2010) Formulation and evaluation of chitosan-based ampicillin trihydrate nanoparticles. *Tropical J Pharmaceutical Res*., 9(5):483-488.
8. Aydin R, Pulat M J. (2012) 5-Fluorouracil encapsulated chitosan nanoparticles for pH-stimulated drug delivery: evaluation of controlled release kinetics. J *Nanomaterials*, 313961-10.
9. Nagarwal R C, Singh P N, Kant S, Maiti P, Pandit J. K. (2011) Chitosan nanoparticles

of 5-fluorouracil for ophthalmic delivery: characterriza-tion, *in-vitro* and *in-vivo* study, *Chem. Pharm. Bull.*, 59(2):272-278.

10. Ummas H, Pratiwi D E, Putri S, Alimin E. (2019) Adsorption study for removal of acid orange dye using modified nano chitosan. IOP Conference Series: *J Physics: Conference Series*., 1244: 01203-01209.
11. Rhazi M, Desbrières J, Tolaimate A, Alagui A, Vincendon M, Vottéro P. (2000) Investigation of different natural sources of chitin Influence of the source and the deacetylation process on the physicochemical characteristics of chitosan. *Polymer International*, 49:337-344.
12. Taha M A, Bounor-Legaré V, de Andrade F N, Do R R, Mckenna L T. (2021) Determination of viscosity average molar masses of polyethylene in a wide range using rheological measurements with a harmless solvent. *Int J Polymer Analysis and Characterization*, 26(7):630-640.
13. Brugnerotto J, Lizardi J, Goyoolea F, Arguelles-Monal W, Desbrieres J, Rinaudo M. (2001) An infrared investigation in relation with chitin and chitosan characterization. *Polymer*, 42:3569–3580.
14. Calvo P, Remunan-Lopez C, Vila-Jato J L, Alonso M J. (1997) Novel hydrophilic chitosan-polyethylene oxide nanoparticles as protein carries. *J Applied Polymer Sci*., 63(1): 125-1321.
15. Mirzadeh H, Yaghobi N, Amanpour S, Ahmadi H, Mohagheghi A, Hormo F. (2002) Preparation of chitosan derived from shrimp's shell of Persian Gulf as a blood hemostasis agent, *Iranian Polymer Science*, 11(1):63-68.
16. Nouri M, Khodaiyan F, Razavi S H, Mousavi M. (2015) Improvement of chitosan production from Persian Gulf shrimp waste by response surface technology. *Food Hydrocolloids*, 3:1-9.
17. Kurita K. (2006) Chitin and chitosan: Functional biopolymers from marine crustaceans, *Material Biotechnology*, 8:203-226.
18. Patria A. (2013) Production and character-rization of chitosan from shrimp shells waste. *AACL Bioflux.*, 6(4):339-344.
19. Brine C J, Sandford P A, Zikakis J P. Advances in Chitin and Chitosan, Elsevier Science Publishers Ltd., London, 1992.
20. Antoniou J, Liu F, Majeed H, Qi J, Yokoyama W, Zhong F. (2015) Physicochemical and morphological properties of size-controlled chitosan–tripolyphosphate nanoparticles. *Colloids and Surfaces A: Physicochemical Eng. Aspects*, 465:137–146.
21. Younes I, Hajji S, Frachet V, Rinaudo M, Jellouli K, Nasri M. (2014) Chitin extraction from shrimp shell using enzymatic treatment: Antitumor, antioxidant and antimicrobial activities of chitosan. *Int J Biology and Macromolecules*, 69:489–498.
22. Pavinatto A, Pavinatto F J, Delezuk J, Nobre T M, Souza A L, Campana-Filho S P, Oliveira O N. (2013) Low molecular-weight chitosans are stronger biomembrane model perturbants, *Colloids, and Surfaces B: Biointerfaces*, 104(1):48-53.
23. Anusha J R, Fleming A T, Valan A M, Chul K B, Al-Dhabi N A, Yu K H, Justin R C. (2016) Mechanochemical synthesis of chitosan submicron particles from the gladius of Todarodes pacificus. *J Advanced Res*., 7:863–871.
24. Hejjaji E M A, Smith A M, Morris G A. Designing chitosan-tripolyphosphate micro-particles with the desired size for specific pharmaceutical or forensic applications. *Int J Biology and Macromolecules*. 2017; 95:564–573.
25. Bangyekan C, Aht-Ong D, Srikulkit K. (2006) Preparation and properties evaluation of chitosan coated cassava starch film. *Carbohydrate Polymer*, 63(1):61-71.
26. Wahab M, Zahoor M, Salman M, Kamran A W, Naz S, Burlakovs J, Kallistova A, Pimenov N, Zekker I. (2021) Adsorption-membrane hybrid approach for the removal of Azithromycin from water: an attempt to minimize drug resistance problem. *Water*, 13:1969-1978.
27. Ciopec M, Davidescu C M, Negrea A, Grozav I, Lupa L, Negrea P, Popa A. (2012) Adsorption studies of Cr(III) ions from aqueous solutions by DEHPA impregnated onto amberlite XAD7 − factorial design analysis. *Chem Eng Res Des*., 90:1660−1670.
28. Hossain M A, Kumita, M, Michigami Y, Mori S. (2005) Kinetics of Cr (VI) adsorption on used black tea leaves. *J Chem Eng Jpn.*, 38:402-406.
29. Ho Y S, McKay G. Kinetics of sorption of divalent metal ions onto sphagnum moss peat. *Water Res.* 2000; 34:735-742.
30. Hossain M A, Alam M S. (2012) Adsorption kinetics of Rhodamine-B on used black tea leaves. *Iran J Environ Health Sci Eng*., 9:2-15.
31. Azam M G, Kabir M H, Shaikh M A A, Ahmed S, Mahmud M, Yasmin S. (2022) A rapid and efficient adsorptive removal of lead

from water using graphene oxide prepared from waste dry cell battery. *J Water Proc Eng*., 46: 102597.
32. Al-Ghouti M A, Al-Absi R S. (2020) Mechanistic understanding of the adsorption and thermodynamic aspects of cationic methylene blue dye onto cellulosic olive stones biomass from wastewater, *Sci Rep*., 10:15928.
33. Munilakshmi N, Srimurali M, Karthikeyan J. (2013) Adsorptive removal of Acid red 1, from aqueous solutions by preformed flocs. *Int J Current Eng. Technol*., 3(4):1456-1462.